

## Correlation of R2 and R2\* with Quantitative Susceptibility Maps in Healthy Elderly Controls

Jeam Haroldo Oliveira Barbosa<sup>1</sup>, Saifeng Liu<sup>2</sup>, Jin Tang<sup>3</sup>, Manju Liu<sup>4</sup>, Weili Zheng<sup>4</sup>, E. Mark Haacke<sup>2,4</sup>, and Carlos Ernersto Garrido Salmon<sup>1</sup>

<sup>1</sup>Department of Physics, University of Sao Paulo, Ribeirao Preto, Sao Paulo, Brazil, <sup>2</sup>School of Biomedical Engineering, McMaster University, Hamilton, Ontario, Canada, <sup>3</sup>MRI Institute for Biomedical Research, Detroit, Michigan, United States, <sup>4</sup>Wayne State University, Detroit, Michigan, United States

**Introduction:** There are a variety of means by which iron content in vivo tissue can be measured. These include but are not limited to measuring: transverse relaxation rates (R2 and R2\*) and quantitative magnetic susceptibility (QSM)<sup>1-3</sup>. However, the dependency of transverse relaxation rates with water content can confound the accuracy of iron quantification if R2 or R2\* are used. To overcome this limitation, magnetic susceptibility mapping has been suggested to evaluate iron deposits in neurodegenerative diseases<sup>4</sup>. We use a specific regularized version of QSM referred to as susceptibility weighted imaging and mapping (SWIM). The correlation between iron concentration and R2, R2\* and SWIM with cadaver brain data have reveals that SWIM and R2\* perform the best<sup>5</sup>. The mechanisms that allow the correlation of SWIM and R2\* with iron content are potentially quite different, with the former representing bulk susceptibility and the latter being more related to the distribution and size of the magnetic sources. In this study, we evaluated the correlation between iron concentration with R2 and R2\* and magnetic susceptibility in vivo in the midbrain region for seven healthy elderly subjects.

**Methods:** Seven healthy controls (age: 64.4±8.6 years) were recruited from the Hospital of Clinicas of University of Sao Paulo (Ribeirao Preto, Brazil). The imaging procedure was performed in a 3T Philips Achieva MRI scanner. For R2 estimation, a Turbo Spin Echo sequence with 16 equally spaced echoes (12-196 ms) was used with TR=3000ms and resolution 0.449x0.449x2.0 mm<sup>3</sup>. For R2\* and SWIM a four echo multi-echo sequence was used (TE=7.7,19.7,31.7,43.7 ms) with TR= 48ms and a resolution 0.479x0.479x2.0 mm<sup>3</sup>. An algorithm was implemented in Matlab to draw ROIs, generate relaxometry maps and extract the mean values for each ROI. Several ROIs were drawn in the midbrain region: substantia nigra (SN), red nucleus (RN), globus pallidus (GP), putamen (PUT), caudate nucleus (CN), white matter (WM), thalamus (THA), gray matter (GM). The R2 values were calculate using Laplace Transform to consider several possible R2 values and for the R2\* a mono-exponential fit was applied. The susceptibility maps were created by first phase unwrapping the data with FSL<sup>7</sup>, then creating a mask to remove the sinuses using the bet2 tool on FSL. A SHARP filter<sup>5</sup> was used to remove background phase contributions (radius 6 mm, regularization parameter 0.05). The resultant phase images were processed using the SWIM algorithm<sup>4</sup> to create susceptibility maps using Matlab (SMART SWIM). The susceptibility value ( $\Delta\chi$ ) was reported here with respect to a certain reference region (WM). The brain iron content for each ROI was calculated based on known formulae as a function of age, except for the SN and RN regions where a mean value estimate was used<sup>6</sup>.

**Results:** Figure 1 shows example SWIM results. All regions and parameters had a significant linear correlation with iron content (Figure 2).

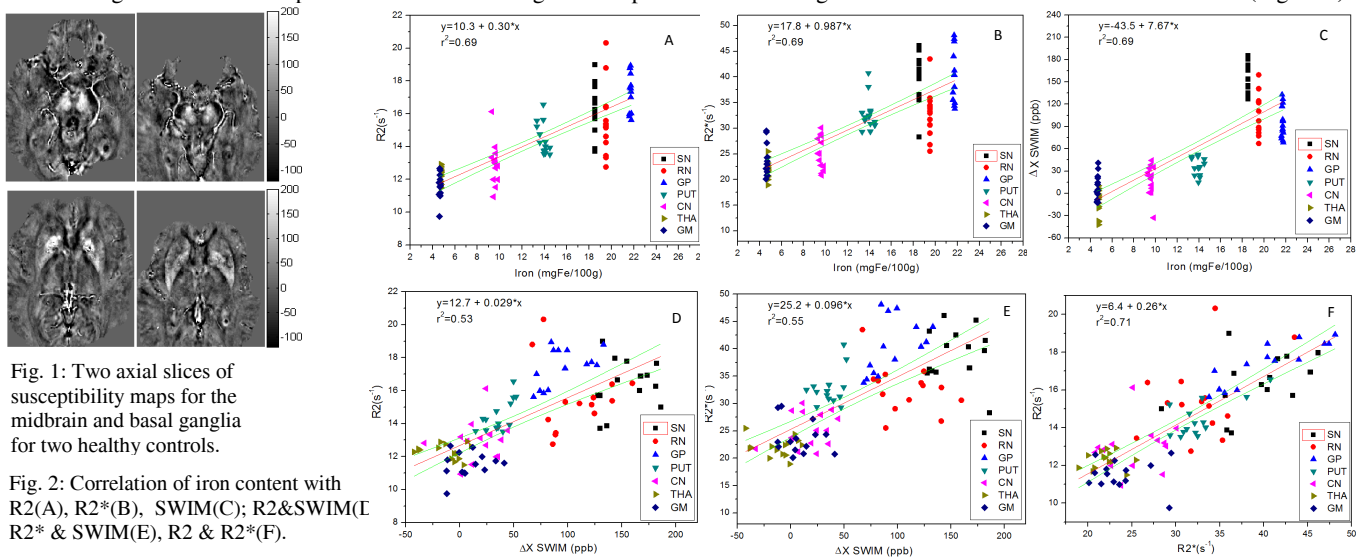


Fig. 1: Two axial slices of susceptibility maps for the midbrain and basal ganglia for two healthy controls.

Fig. 2: Correlation of iron content with R2(A), R2\*(B), SWIM(C), R2&SWIM(D), R2\* & SWIM(E), R2 & R2\*(F).

**Discussion:** For correlation between R2 and iron, we found at 3T the proportional correlation parameters ( $y=0.30*x+10.3$ ,  $r^2=0.69$ ). This is to be compared to the results of Vyamazal et al<sup>1</sup> ( $y=0.19*x+10.3$ ,  $r^2=0.83$ ). The difference is likely because these authors used lower field (1.5T) suggesting that there is an increased R2 sensitivity at higher field. (Only one subject showed more than one R2 value in any given region which isn't in concordance with some reports<sup>1,11</sup> but also doesn't affect the results reported herein). For the correlation between R2\* and iron content for GP, SN, RN, PUT, CN, WM, we found almost the same correlation parameters ( $y=0.96*x+18.2$ ,  $r^2=0.61$ ) compared to Martin et al<sup>9</sup> ( $y=1.0*x+17.5$ ,  $r^2=0.81$ ). In the more restricted regions of just GP, PUT, THA and CN, we found the same correlation parameters ( $y=1.1*x+16.0$ ,  $r^2=0.80$ ) as Yao et al<sup>8</sup> ( $y=1.2*x+14.2$ ,  $r^2=0.87$ ). The R2 and R2\* values of WM were very similar to those found in GM e THA. The linear slope between susceptibility and iron content was (7.7 ppb/mgFe/100g) close to Wharton et al<sup>10</sup> (7.5ppb/mgFe/100g) that used multiple orientations. For intercorrelation of the different MRI techniques, the highest correlation coefficient was observed in the comparison between the relaxometry parameters. The susceptibility measurements introduced some dispersion in the data, maybe influenced by some of the recognized problems of the technique such as the relative nature of susceptibility and the orientation influence<sup>5</sup>.

**Conclusion:** R2, R2\* and  $\Delta\chi$  show similar correlation with iron content in the midbrain region, but the R2 and R2\* measurements appear to be more sensitive to low iron content. The results presented here are in agreement with other recent work in this area<sup>1,5,8-11</sup>.

**References:** 1. Vyamazal J. et al. Radiology, 211: 489-495. 1999. 2. Shmueli, K., et al. 2009. Magn. Reson. Med. 62, 1510-1522. 3. Wharton, S., Bowtell, R., 2010. Neuroimage 53, 515-525. 4. Haacke E.M. et al. (2010) J Magn Reson Imagin 32:663-676. 5. Langkammer C. et al. (2012). Neuroimage 62, 1593-1599. 6. Hallgren B. and Sourander P., (1958), J. Neurochem. 3, 41-51. 7. Jenkinson, M., 2003. Magn. Reson. Med. 49 (1), 193-197. Radiology, 211(2):489-495. 8. Yao B., et al. (2009). Neuroimage, 44:1259-1266. 9. Martin et al. (2008). Neurology 70:1411-17. 10. Wharton S. and Bowtell R., (2010). Neuroimage 53, 515-525. 11. Langkammer C. et al. (2010). Radiology 257(2), 455-462.